

IR Chemiluminescence Probe of the Vibrational Energy Distribution of CO₂ Formed during Steady-State CO Oxidation on Pt(111) and Pt(110) Surfaces

Kenji Nakao, Shin-ichi Ito, Keiichi Tomishige,^{*,†} and Kimio Kunimori^{*,‡}

Institute of Materials Science, University of Tsukuba, 1-1-1 Tennodai, Tsukuba, Ibaraki 305-8573, Japan

Received: August 26, 2005; In Final Form: October 11, 2005

The infrared (IR) chemiluminescence spectra of CO₂ were measured during the steady-state CO + O₂ reaction over Pt(110) and Pt(111) surfaces. Analysis of the IR emission spectra indicates that the bending vibrational temperature (T_V^B), as well as the antisymmetric vibrational temperature (T_V^{AS}), was higher on Pt(110) than on Pt(111). On the Pt(110) surface, the highly excited bending vibrational mode compared to the antisymmetric vibrational mode was observed under reaction conditions at low CO coverage ($\theta_{CO} < 0.2$) or at high surface temperatures ($T_S \geq 700$ K). This can be related to the activated complex of CO₂ formation in a more bent form on the inclined (111) terraces of the Pt(110)(1 × 2) structure. On the other hand, at high CO coverage ($\theta_{CO} > 0.2$) or at low surface temperatures ($T_S < 650$ K), T_V^{AS} was higher than T_V^B , which can be caused by the reconstruction of the Pt(110)(1 × 2) surface to the (1 × 1) form with high CO coverage.

1. Introduction

Elucidation of the reaction mechanism is important for catalyst design and control of reaction routes. Single-crystal surfaces can be used to elucidate reaction mechanisms over heterogeneous catalysts.^{1–11} An effective method is spectroscopic observation of reaction intermediates, which are surface species in a metastable state, to obtain information about the reaction mechanism.^{9–11} Another method is investigation of internal (vibrational and rotational) energy and translational energy of desorbed molecules, which are the products of catalytic reaction, from the catalyst surface.^{12–29} The energy states of desorbed molecules can reflect the catalytic reaction dynamics, which can correspond to a transition state (i.e., structure of the activated complex).^{12–29} Numerous investigations of CO oxidation on Pt and Pd surfaces have revealed the elemental steps of surface-catalyzed reactions.^{1–29} Furthermore, CO oxidation is a prototype reaction for the study of dynamics; measurements of internal energy states of the produced CO₂ molecules have been performed using an infrared chemiluminescence (IR emission) method under steady-state catalytic reactions using a molecular-beam technique.^{13–25} Analyses of vibrational states can yield information about the structure of the activated CO₂ complex (i.e., the dynamics of CO oxidation) from which the gas-phase molecules desorbed. Furthermore, the vibrational energy states of product CO₂ depend on its surface structure.^{17–25} Consequently, information about the active sites is obtainable from the IR emission spectra of CO₂ under a steady-state catalytic reaction.

Brown and Bernasek¹² and Mantell et al.^{13,14} studied the IR chemiluminescence during CO oxidation on polycrystalline Pt surfaces and reported that the product CO₂ molecules were vibrationally excited substantially beyond thermal equilibrium with the surface. Coulston and Haller¹⁵ studied the dynamics of CO oxidation on polycrystalline Pd, Pt, and Rh surfaces by

measuring high-resolution IR emission spectra and reported that the apparent vibrational temperatures are in the same order as the peak reaction rates, that is, Pd > Pt > Rh. Our group has reported IR chemiluminescence of CO₂ from the steady-state CO + O₂ reaction on single-crystal Pt and Pd surfaces combined with kinetic results.^{17–19,21,23,25} The activated complex of CO₂ formation (the transition state of CO₂ formation from CO(a) + O(a)) has a more bent structure on Pd(111) and a less bent structure on Pd(110) at higher surface temperatures ($T_S > 600$ K), because the bending vibration was more excited for CO₂ from Pd(111) and the antisymmetric vibration was more excited for CO₂ from Pd(110).^{19,23,25} In contrast, at lower temperatures ($T_S = 550$ – 600 K) and in a high CO coverage region, the antisymmetric vibration is very highly excited on both Pd surfaces, which can be related to the activated complex of CO₂ formation in a more linear form.^{21,23,25} For single-crystal Pt surfaces, Watanabe et al.^{17,18} reported that the vibrational states of the product CO₂ molecules were more excited on Pt(110) than on Pt(111). At that time, however, only information on an average vibrational temperature (T_V^{AV}) was obtained.¹⁸

A clean Pt(110) surface is reconstructed into a (1 × 2) missing-row structure above 275 K, and the reconstruction is lifted to the (1 × 1) form by CO(a). It starts at about $\theta_{CO} = 0.2$ and is completed at $\theta_{CO} = 0.5$.¹ These two structures yield differently oriented oxygen adsorption sites,^{30,31} and the product CO₂ desorbs into different directions from the results of angle-resolved (AR) measurements.^{26,27} The (1 × 2) reconstructed surface consists of three-atom-wide (111) terraces declining about 30° into the [001] direction. Desorbing product CO₂ from this surface showed well-split two-directional desorptions colimated $\pm 25^\circ$ off the surface normal into the [001] direction.^{26,27} On the other hand, CO₂ from the (1 × 1) structure is desorbed along the surface normal.^{26,27}

In this work, we have studied the dynamics of CO₂ formation during the CO oxidation over single-crystal Pt(110) and Pt(111) surfaces. Recently, we modified the apparatus, and this has enabled observation under more severe conditions (i.e., with lower CO₂ formation rates at lower surface temperatures).^{21,23,25} Furthermore, more detailed analysis of IR emission spectra has

* Authors to whom correspondence should be addressed.

† E-mail: tomi@tulip.sannet.ne.jp.

‡ Tel: +81-29-853-5026. Fax: +81-29-855-7440. E-mail: kunimori@ims.tsukuba.ac.jp.

been possible using the IR intensity.^{21–25} It is the first presentation that the detailed analyses of vibrational energy states of the produced CO₂ molecules give information about the dynamics of CO₂ formation, which are changed by lifting the surface structure of Pt(110).

2. Experimental Section

A molecular-beam reaction system, in combination with a FT-IR spectrometer (InSb detector Nexus670; Thermo Electron Corp.), was used to measure IR emissions of product CO₂ molecules that desorbed from the metal surface during catalytic reactions.^{19–25} A UHV chamber (base pressure < 1.0 × 10^{−9} Torr) was equipped with a CaF₂ lens, which collected IR emission; an Ar⁺ ion gun for sample cleaning; and a quadrupole mass spectrometer (QMS, QME200; Pfeiffer Vacuum Technology AG) with a differential pumping system. Two free-jet molecular-beam nozzles (0.1-mm diameter orifice) supplied the reactant gases. The reactant fluxes were controlled by mass-flow controllers. The CO and O₂ gases (the total flux of 8.1 × 10¹⁸ cm^{−2} s^{−1}; CO/O₂ = 0.33–3.0) were exposed to single-crystal Pt surfaces (Pt(110) and Pt(111)). Steady-state CO + O₂ reactions were performed at temperatures of 500–900 K. Another UHV chamber (base pressure < 2.0 × 10^{−10} Torr) was used to prepare the samples and to characterize Pt(110) and Pt(111) surfaces. It was equipped with an identical molecular-beam reaction system, an Ar⁺ ion gun, low-energy electron diffraction (LEED), and a QMS. Before the molecular-beam reaction, the Pt(110) and Pt(111) surfaces were cleaned using a standard procedure (O₂ treatment, Ar⁺ bombardment, and annealing).^{19–25} After cleaning, the sharp reconstructed (1 × 2) and (1 × 1) LEED patterns were observed for Pt(110) and Pt(111), respectively.

The IR emission spectra of the CO₂ molecules desorbed from the surface were measured with 4-cm^{−1} resolution. At that low resolution, no individual vibration–rotation lines were resolved. The spectra were analyzed on the basis of simulations of model spectra.^{14,16} They yielded an average vibrational Boltzmann temperature (T_V^{AV} : an average temperature of antisymmetric stretch, symmetric stretch, and bending modes), which could be calculated from the degree of the red-shift from the fundamental band (2349 cm^{−1}).^{14,16,23} Although the IR emission observed here is in the antisymmetric stretch vibrational region—(n_{SS}, n_B^l, n_{AS}) → ($n_{SS}, n_B^l, n_{AS} - 1$), the vibrational excitation levels of symmetric stretch (n_{SS}) and bending (n_B) also affect this region.^{14,19} Here, n_{SS} , n_B , and n_{AS} are the vibrational quantum numbers of respective modes. The quantum number of vibrational angular momentum in linear molecules is denoted by l . Note that the emission intensity is normalized using the rate of CO₂ production. Consequently, the emission intensity is related to the extent of excitation in the antisymmetric stretch of CO₂, which is given by following equation:

$$f \propto \exp(-\Delta E_V / k_B T_V^{AS}) \quad (1)$$

where f is the emission intensity normalized per unit of CO₂ yield, ΔE_V is the energy spacing, k_B is the Boltzmann constant, and T_V^{AS} is the antisymmetric vibrational temperature. Therefore, T_V^{AS} can be estimated from the normalized emission intensity.^{21–25} On the basis of T_V^{AS} and T_V^{AV} , it is possible to deduce the bending vibrational temperature (T_V^B). The relation between T_V^{AV} and respective vibrational temperatures is represented as

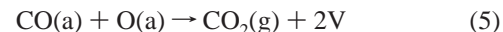
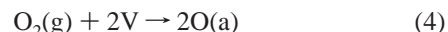
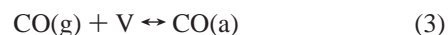
$$T_V^{AV} = (T_V^{AS} + T_V^{SS} + 2T_V^B)/4 \quad (2)$$

TABLE 1: Kinetic Parameters for CO Oxidation on Pt(110)

reaction equation	rate constant/s ^{−1}	ν/s^{-1}	$E_a/kcal\ mol^{-1}$	ref
(3)	k_{CO}^{des}	2×10^{16}	36.2	[32,33]
reaction equation	initial sticking coefficient			ref
(3)	$s_{CO} = 0.83$			[34]
(4)	$s_{O_2} = 0.4$			[35]
reaction equation	saturation coverage			ref
(3)	$\theta_{CO,S} = 1.0$			[36]
(4)	$\theta_{O,S} = 0.35$			[35]

where $2T_V^B$ corresponds to the degeneration of the bending vibration. Assuming that T_V^B is equal to T_V^{SS} because of the Fermi resonance,^{15,29} T_V^B is expected to be $(4T_V^{AV} - T_V^{AS})/3$. This assumption is plausible on the basis of previous reports.^{14,15,29} It should be added that T_V^{AV} , T_V^{AS} , and T_V^B were used here as parameters to characterize the extent of the vibrational excitation of the product CO₂. About 30–60 min were required to measure the IR spectra with 2000–4000 scans. The activity was stable during measurement. Therefore, we infer that the results reflected the CO₂ states under steady-state conditions.

To estimate the coverages of CO (θ_{CO}) and oxygen (θ_O) under steady-state conditions, we considered the mechanism and the differential equations. As is known well, the mechanism of the CO oxidation on the Pt surface is as follows:^{1–3}



where V is a vacant site. It is possible to write the equations regarding the coverage of each intermediate as shown below:³²

$$d\theta_{CO}/dt = f_{CO} s_{CO} [1 - (\theta_{CO}/\theta_{CO,S})^3] - k_{CO}^{des} \theta_{CO} - r_{CO_2} \quad (6)$$

$$d\theta_O/dt = 2f_{O_2} s_{O_2} (1 - \theta_{CO}/\theta_{CO,S} - \theta_O/\theta_{O,S})^2 - r_{CO_2} \quad (7)$$

where f and s are the flux of reactants to the surface and the initial sticking coefficients, respectively. The k_{CO}^{des} is the rate constant for CO desorption. The rate of O₂ desorption is assumed to be small enough to be neglected.^{18,32} The subscript S denotes saturation. The CO₂ formation rate, r_{CO_2} , was obtained from experimental results. The initial sticking coefficients of CO and O₂, kinetic parameters, and saturation coverage used are listed in Table 1. More strictly, one should take into account that the activation energy of CO desorption and the (1 × 2) ↔ (1 × 1) phase transition depend on the coverages. However, we have used the above equations to estimate the surface coverages approximately.

3. Results and Discussion

Figure 1 shows the rate of CO₂ formation in the steady-state CO + O₂ reaction on Pt(110) and Pt(111) as a function of surface temperature (T_S) (CO/O₂ = 1). The CO oxidation proceeded above 550 K, and the profiles of the formation rate had a maximum on both surfaces. The behavior agrees well with the general Langmuir–Hinshelwood (LH) kinetics of CO oxidation on Pt surfaces.^{1–3,17,18} It is known that at lower surface temperatures, the surface coverage of CO is high, and the rate-determining step is O₂ adsorption on the vacant site, which is

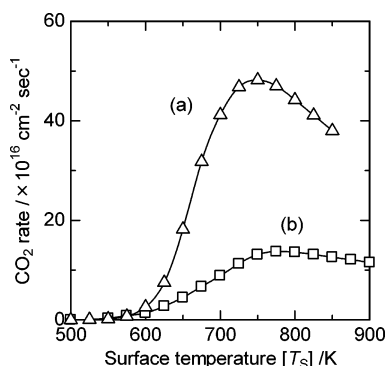


Figure 1. The formation rate of CO_2 during the $\text{CO} + \text{O}_2$ reaction ($\text{CO}/\text{O}_2 = 1$) on (a) Pt(110) and (b) Pt(111). The total flux of reactants ($\text{CO} + \text{O}_2$) was $8.2 \times 10^{18} \text{ molecules cm}^{-2} \text{ s}^{-1}$.

formed by the desorption of CO(a). At higher surface temperatures, the formation rate of CO_2 decreased gradually with increasing surface temperature, and this behavior is due to the decrease of CO coverage. The temperature at which the highest activity was obtained is denoted as T_s^{max} . Obviously, the activity for CO oxidation and T_s^{max} is different between Pt(110) and Pt(111) surfaces. These results show that the CO oxidation on Pt surfaces is structure-sensitive in the kinetics under the steady-state reaction condition. The differences may depend on the difference of the coverage of oxygen and CO during the steady-state reaction. Especially, the sticking coefficient of oxygen may be different between these surfaces. For example, an initial sticking coefficient (s_0) of O_2 is 0.4 on Pt(110)³⁵ and 0.048 on Pt(111).³⁷ It has been reported in some cases that CO oxidation on Pt(110) exhibits oscillation.^{3–8} However, we did not observe the phenomenon, because the experimental conditions such as reactant pressures and temperatures differ from our conditions.

Figure 2 parts a and b, show IR emission spectra of CO_2 molecules produced by the $\text{CO} + \text{O}_2$ reaction on Pt(110) and Pt(111) surfaces ($\text{CO}/\text{O}_2 = 1$) for various surface temperatures. The CO_2 emission spectra observed in the region of $2400\text{--}2150 \text{ cm}^{-1}$ are considerably red-shifted from 2349 cm^{-1} (fundamental band of antisymmetric stretch). On Pt(110) at $T_s \geq 700 \text{ K}$, the higher the surface temperature, the greater the red-shift from the antisymmetric stretch fundamental (2349 cm^{-1}) observed in the CO_2 emission spectra, even though the emission intensity is almost constant. On the other hand, at low

surface temperatures ($T_s < 700 \text{ K}$), the lower the surface temperature, the greater the red-shift from 2349 cm^{-1} , and the emission intensity increased with decreasing T_s .

Figure 3 shows the average vibrational temperature (T_V^{AV}) on Pt(110) and Pt(111) surfaces derived from the IR emission spectra of CO_2 as a function of T_s . The T_V^{AV} value was much greater than that of T_s , which indicates that the product CO_2 is vibrationally excited. The T_V^{AV} values on Pt(110) higher than on Pt(111) are in good agreement with the results of Watanabe et al.^{17,18} The T_V^{AV} value increases with increasing T_s at high temperatures ($T_s \geq 700 \text{ K}$) on both surfaces. This is related to the exothermic reaction heat, which can be distributed to translational and internal (vibrational and rotational) energies of desorbed molecules, and it can also be distributed to the surface.^{27,38} It is thought that the energy distribution to the surface can become lower at the higher surface temperatures.²⁵ On the other hand, the T_V^{AV} value on Pt(110) increases with decreasing T_s at low temperatures of $625\text{--}700 \text{ K}$, indicating that the vibrational states of the desorbed CO_2 are changed at around 700 K on Pt(110). Watanabe et al.¹⁸ suggested that the T_V^{AV} value increased as the coverage of CO increased at the lower T_s . Figure 4, parts a and b, shows T_V^{AS} and T_V^{B} derived from the IR emission intensity of CO_2 as a function of T_s . For surface temperatures above 700 K , the T_V^{B} value increases gradually with increasing T_s on both surfaces. Especially, the T_V^{B} values are much higher than those of T_V^{AS} at the higher T_s , meaning that the bending vibrational mode is more highly excited than the antisymmetric vibrational mode on both surfaces at the higher T_s . The structure of the activated complex of CO_2 formation can be discussed from the experimental results.

In our previous reports, the structure of the activated complex in CO oxidation on Pd(111) is more bent than that on Pd(110) on the basis of the analysis of the vibrational excitation states of the product CO_2 .^{19,20,23,25} This behavior can be explained by the flat Pd(111) surface on an atomic scale. In the case of Pt(111), the bending vibration was more excited than the antisymmetric vibration, and this can also be due to the flat surface structure. However, the bending vibrational temperature is much higher on Pd(111) ($T_V^{\text{B}} = 2200 \text{ K}$ at $T_s = 800 \text{ K}$)²³ than on Pt(111) ($T_V^{\text{B}} = 1750 \text{ K}$ at $T_s = 800 \text{ K}$, as shown in Figure 4b). The higher vibrational temperatures on Pd(111), compared to Pt(111), are in good agreement with the results of Coulston and Haller,¹⁵ although polycrystalline Pd and Pt foils were used.

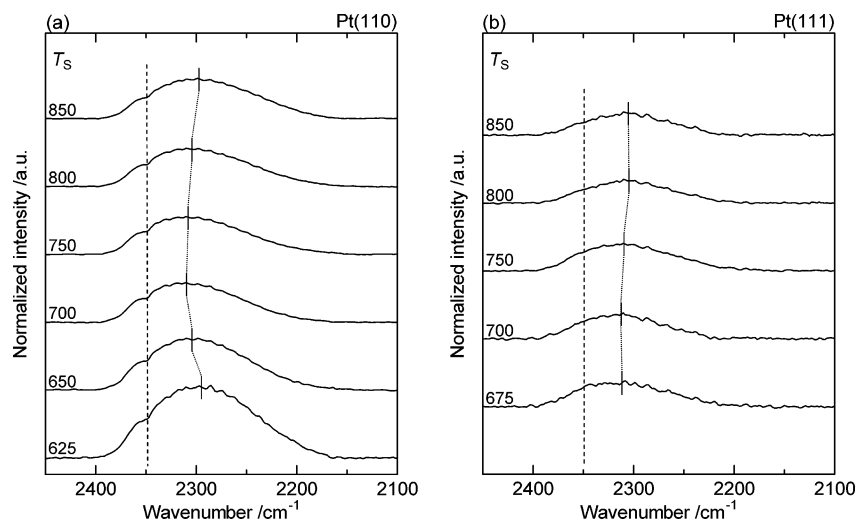


Figure 2. IR emission spectra of CO_2 desorbed by the $\text{CO} + \text{O}_2$ reaction on (a) Pt(110) and (b) Pt(111). The surface temperature (T_s) was $625\text{--}850 \text{ K}$. The flux conditions are as described in Figure 1. The IR emission spectrum centered at 2143 cm^{-1} of the nonreacted CO was subtracted.^{15,16} The emission intensity was normalized per unit of CO_2 yield.

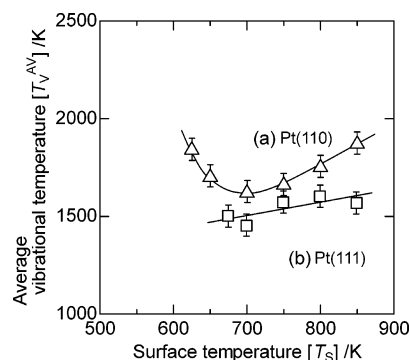


Figure 3. Surface temperature dependence of the average vibrational temperature (T_V^{AV}) of CO₂ formed in the CO + O₂ reaction on (a) Pt(110) and (b) Pt(111). The flux conditions are as described in Figure 1.

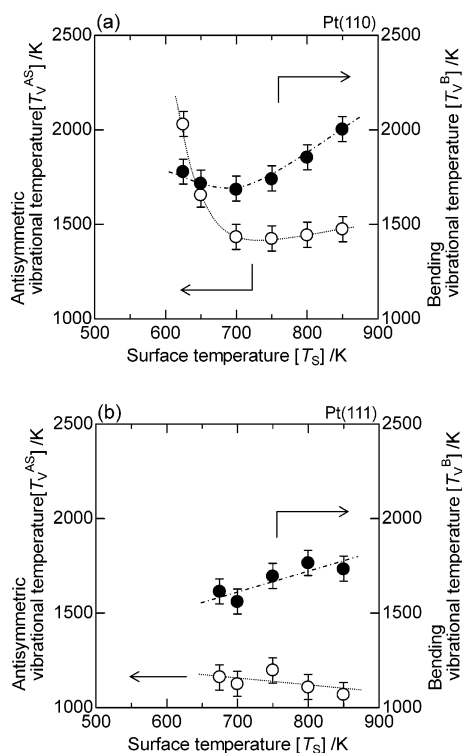


Figure 4. Surface temperature dependence of the antisymmetric vibrational temperature (T_V^{AS}) and the bending vibrational temperature (T_V^B) on (a) Pt(110) and (b) Pt(111). The flux conditions are as described in Figure 1.

They argued that the excess bending in the case of Pd might be due to the higher density of states at the Fermi level in the case of Pd compared to Pt.¹⁵

In the case of Pt(110), at surface temperatures higher than 700 K, the bending vibration was also more excited than the antisymmetric vibration (Figure 4a). This behavior does not agree with that on Pd(110).^{19–21,23,25} Both T_V^B and T_V^{AS} values are higher on Pt(110) than on Pt(111) (Figure 4), while T_V^B was higher on Pd(111) than on Pd(110), and T_V^{AS} was higher on Pd(110) than on Pd(111) at higher surface temperatures.²³ As is well-known, the Pt(110)(1 × 1) surface can be reconstructed to the Pt(110)(1 × 2) surface, and the reconstruction behavior is dependent on the CO coverage.^{1,27} In contrast, this kind of reconstruction on Pd(110) has not been reported. These different tendencies can explain the difference in the vibrational excitation states of the product CO₂ over Pt(110) and Pd(110), and this suggests that the difference can be caused by the reconstruction of the Pt(110) surface. In the case of Pt(110), it

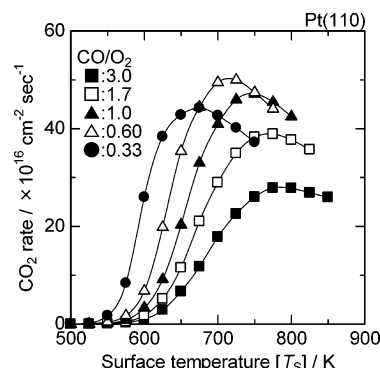


Figure 5. The formation rate of CO₂ during the CO + O₂ reaction (CO/O₂ = 0.33–3.0) on Pt(110). The total flux of reactants (CO + O₂) was $8.2 \times 10^{18} \text{ molecules cm}^{-2} \text{ s}^{-1}$.

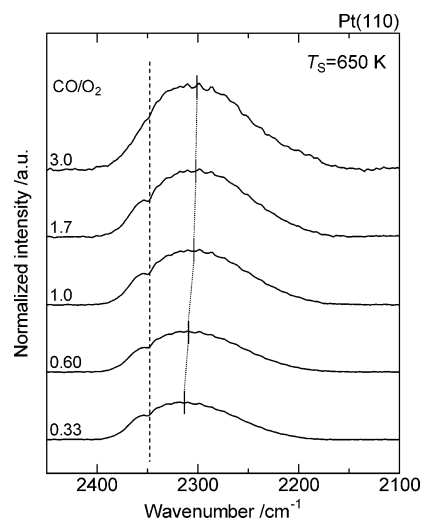


Figure 6. IR emission spectra of CO₂ desorbed by the CO + O₂ reaction on Pt(110). The surface temperature (T_S) was 650 K. The flux conditions are as described in Figure 5. The IR emission spectrum centered at 2143 cm^{-1} of the nonreacted CO was subtracted.^{15,16} The emission intensity was normalized per unit of CO₂ yield.

is expected that the surface structure is reconstructed into the (1 × 2) form because of low CO coverage ($\theta_{\text{CO}} < 0.03$ at $T_S \geq 700 \text{ K}$). On the other hand, the excited state of CO₂ was different at lower T_S . As shown in Figure 4a, the T_V^{AS} value increases drastically with decreasing T_S at temperatures below 700 K, indicating that the vibrational states of the desorbed CO₂ are changed at around 700 K on Pt(110). At lower temperatures such as 625 and 650 K, the coverage of CO can be rather high, and the high CO coverage can stabilize Pt(110)(1 × 1). On the basis of the coverage estimation, the coverage of CO (θ_{CO}) is calculated to be 0.25 and 0.62 at $T_S = 650$ and 625 K, respectively. The result suggests that the change in the vibrational states is related to the reconstruction of Pt(110)(1 × 2) to the (1 × 1) form with the higher θ_{CO} . To elucidate the effect of the coverage of CO and oxygen more clearly, we investigated the dependence of the CO/O₂ ratio at a fixed surface temperature.

Figure 5 shows the CO₂ formation rate in the steady-state CO + O₂ reaction on Pt(110) as a function of surface temperature (T_S) for various CO/O₂ ratios. The total flux of reactants was constant at $8.2 \times 10^{18} \text{ cm}^{-2} \text{ s}^{-1}$ in all these experiments. The temperature dependence of the curves shows maxima: the observed behavior resembles that shown in Figure 1. In Figure 5, T_S^{max} increased significantly with an increase in the CO/O₂ ratio. These behaviors also agree well with the general LH kinetics of CO oxidation on Pt surfaces.^{1–3,17,18} On

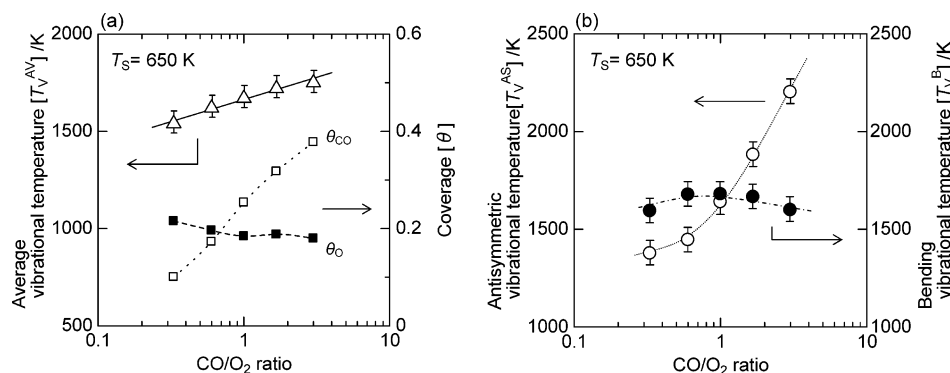


Figure 7. (a) CO/O₂ ratio dependence of the average vibrational temperature (T_V^{AV}) of CO₂ formed in the CO + O₂ reaction on Pt(110) and the coverages of CO and oxygen. (b) CO/O₂ ratio dependence of the antisymmetric vibrational temperature (T_V^{AS}) and the bending vibrational temperature (T_V^B). The flux conditions are as described in Figure 5.

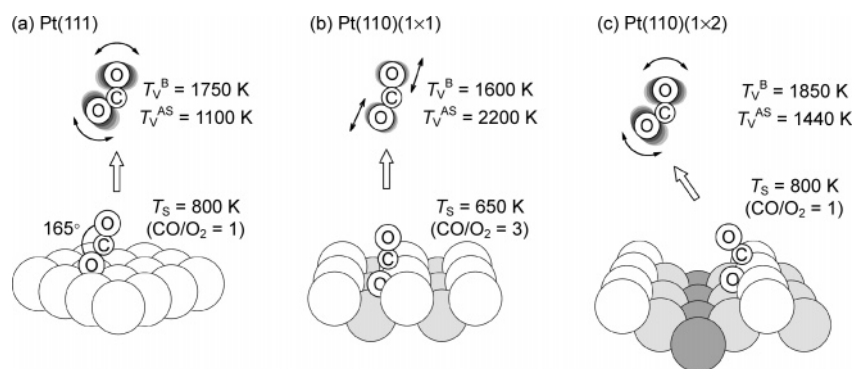


Figure 8. Structure of the activated complex of CO₂ formation and the vibrationally excited states of the desorbed CO₂ molecules: (a) Pt(111), (b) Pt(110)(1 × 1), and (c) Pt(110)(1 × 2).

the basis of the results of CO₂ formation rate, the surface temperature was fixed at 650 K, where the IR emission spectra were obtained.

Figure 6 depicts the IR emission spectra of CO₂ molecules produced by the CO + O₂ reaction on Pt(110) at $T_S = 650$ K for various CO/O₂ ratios. The higher the CO/O₂ ratio, the larger is the red-shift from 2349 cm⁻¹ observed in the CO₂ emission spectra. In addition, the emission intensity became larger with an increase in the CO/O₂ ratio. Figure 7a shows T_V^{AV} obtained from the IR emission spectra of CO₂. The coverages of adsorbed CO and oxygen as a function of the CO/O₂ ratio obtained from the calculation are also shown in Figure 7a. The T_V^{AV} value increased slightly with an increase in the CO/O₂ ratio. Figure 7b shows T_V^{AS} and T_V^B obtained from the IR emission intensity of CO₂ as a function of the CO/O₂ ratio. In the low CO/O₂ region, the T_V^{AS} value is lower than T_V^B , although the T_V^B values are almost constant with a change in the CO/O₂ ratio. In contrast, T_V^{AS} increased sharply in the higher CO/O₂ region. Therefore, the T_V^{AS} values were much higher than the T_V^B values in the high CO/O₂ region. These behaviors are consistent with those obtained from the results of the T_S dependence shown in Figure 4. From the comparison between θ_{CO} and T_V^{AS} , T_V^{AS} drastically increased in the range of $\theta_{CO} > 0.2$. Considering that the Pt(110)(1 × 2) surface is reconstructed to the (1 × 1) form induced by the CO adsorption above $\theta_{CO} = 0.2$, it is suggested again that the observed phenomenon is strongly related to the reconstruction.

On the basis of the excited states of vibrational modes given from the analysis of the IR emission spectra, the models of the activated complex of CO₂ formation are discussed. Figure 8 illustrates the models of the activated CO₂ complex formed from the adsorbed CO(a) and O(a) species. A stable adsorption site of O(a) is a 3-fold hollow site, and that of CO(a) is an on-top

site on Pt(111).^{39,40} On the basis of these stable adsorption sites of CO(a) and O(a) on Pt(111), the angle of O-C-O in the activated complex of CO₂ formed from these adsorbed species was thought to be bent, and this interpretation has been applied in the CO + O₂ reaction on Pd(111).^{19,20,23,25} However, the T_V^B value (e.g., 1750 K) lower than that on Pd(111) (2200 K)^{23,25} suggests that the activated CO₂ complex is less bent on Pt(111). Mantell et al.^{13,14} estimated the angle of O-C-O to be 165° from the T_V^B value of 1750 K. Therefore, we used this angle to illustrate the activated complex on Pt(111) (Figure 8a). On the other hand, in the case of Pt(110)(1 × 1), the stable adsorption site of CO(a) is an on-top site in the first layer,^{31,41} and that of O(a) is a 3-fold hollow site between the first and second layers.^{31,42,43} The lower T_V^B value ($T_V^B = 1600$ K at $T_S = 650$ K, CO/O₂ = 3) suggests that the angle of O-C-O of the activated complex can be more linear than 165°. The characteristic point is that the very high T_V^{AS} value was observed on the Pt(110)(1 × 1) surface. Similar effects of the high CO coverage on the antisymmetric vibration were also observed on Pd(111) and Pd(110) at lower T_S .^{21,23,25} The activated complex can be formed by the adsorbed CO mounting on the adsorbed oxygen atom (Figure 8b). Besides, Zhdanov⁴⁴ has shown that the change in the energy distribution of the reaction products with increasing coverage can be related to lateral adsorbate-adsorbate interactions in the activated state for reaction. Under the condition of low CO coverage ($\theta_{CO} < 0.2$), the reconstructed Pt(110)(1 × 2) surface is stable.¹ On the Pt(110)(1 × 2) surface, the most stable adsorption site of oxygen atom is a 4-fold hollow site of Pt(110)(1 × 2) missing row troughs,^{31,42,43} and it has been known that the oxygen atoms can also be adsorbed on a 3-fold hollow site on the (111) declining terraces of Pt(110)(1 × 2),^{31,42,43} although the adsorption energy of this site was a little lower than that of the 4-fold hollow site. The adsorption

site of CO is usually an on-top site in the first layer of Pt(110)-(1 × 2). The activated CO₂ complex can be more bent on the Pt(110)(1 × 2) surface, because T_V^B was higher than that on Pt(111). The reaction sites of the CO₂ formation may be not only the terrace of the (111) structure, but also trough and/or topmost Pt atoms. According to the AR measurement, however, Matsushima et al.^{26,27} have shown that CO₂ desorption splits into two inclined components collimating at $\pm 25^\circ$ in the plane along the [001] direction. These results suggest that the activated complex is formed on the inclined (111) terrace in a more bent form (Figure 8c). Although the inclined terrace has a nominal (111) structure, the geometric environment⁴⁵ and/or the electronic states of the inclined surface may be different from those of the usual Pt(111) surface, because only the two-atom-wide (111) terraces are available for the adsorbates (Figure 8c).

Recently, it was suggested that CO oxidation on Pt occurs via a hot-precursor mechanism.⁴⁶ On the other hand, the other recent study⁴⁷ doubts this suggestion. In the CO + O₂ reaction on Pt and Pd surfaces, it has been considered that the adsorbed CO and oxygen are accommodated to the surface before the CO(a) + O(a) reaction.^{12–25} In other words, the lifetime of CO(a) and O(a) is long enough to be accommodated to the surface¹ (the typical LH mechanism). On the other hand, in the CO + NO reaction on Pd(110) at high surface temperatures, we have observed more vibrationally excited CO₂ molecules.^{22,24} Therefore, we have proposed that hot oxygen from NO dissociation, which reacts with CO immediately after the formation, can affect the extent of the vibrational excitation.^{22,24}

4. Conclusions

The steady-state activity of the CO + O₂ reaction over Pt(110) and Pt(111) surfaces was measured in the temperature range of 500–900 K, and the IR chemiluminescence of CO₂ formed during the reaction was studied. From the analysis of the IR emission spectra on Pt(111), T_V^B was found to be lower than that on Pd(111), indicating that the activated complex of CO₂ formation is less bent on Pt(111) than on Pd(111). Both T_V^B and T_V^{AS} values were higher on Pt(110) than on Pt(111). On the Pt(110) surface, T_V^{AS} was higher than T_V^B at lower surface temperatures ($T_S < 700$ K). On the other hand, T_V^B became higher than T_V^{AS} at the higher T_S range (≥ 700 K), where the Pt(110) surface had the reconstructed (1 × 2) structure. The dependence of the CO/O₂ ratio at $T_S = 650$ K showed that T_V^{AS} was much higher than T_V^B at the higher CO/O₂ ratios, suggesting that the Pt(110)(1 × 2) surface was reconstructed to the (1 × 1) form with high CO coverage. At lower CO/O₂ ratios, the activated complex was formed in a more bent form on the declining (111) terrace of the Pt(110)(1 × 2) surface.

Acknowledgment. This work was supported by the 21st Century Center of Excellence (COE) Program of the Ministry of Education, Culture, Sports, Science and Technology (MEXT), Japan.

References and Notes

- (1) Ertl, G. *Adv. Catal.* **1990**, 37, 213.
- (2) Nieuwenhuys, B. E. *Adv. Catal.* **1999**, 44, 259.
- (3) Imbihl, R.; Ertl, G. *Chem. Rev.* **1995**, 95, 697.
- (4) Zhdanov, V. P. *Surf. Sci. Rep.* **2002**, 45, 231.
- (5) Thostrup, P.; Kruse Vestergaard, E.; An, T.; Lægsgaard, E.; Besenbacher, F. *J. Chem. Phys.* **2003**, 118, 3724.
- (6) Hendriksen, B. L. M.; Frenken, J. W. M. *Phys. Rev. Lett.* **2002**, 89, 046101.
- (7) Oertzen, A. v.; Rotermund, H. H.; Milkhaïlov, A. S.; Ertl, G. *J. Phys. Chem. B* **2000**, 104, 3155.
- (8) Carlsson, P.-A.; Zhdanov, V. P.; Kasemo, B. *Appl. Surf. Sci.* **2005**, 239, 424.
- (9) Xu, J.; Yates, J. T. Jr. *J. Chem. Phys.* **1993**, 99, 725.
- (10) Yoshinobu, J.; Kawai, M. *J. Chem. Phys.* **1995**, 103, 3220.
- (11) Nakai, I.; Kondoh, H.; Amemiya, K.; Nagasaka, M.; Shimada, T.; Yokota, R.; Nambu, A.; Ohta, T. *J. Chem. Phys.* **2005**, 122, 134709.
- (12) Brown, L. S.; Bernasek, S. L. *J. Chem. Phys.* **1985**, 82, 2110.
- (13) Mantell, D. A. Ph.D. Thesis, Department of Physics, Yale University, New Haven, CT, 1983.
- (14) Mantell, D. A.; Kunimori, K.; Ryali, S. B.; Haller, G. L.; Fenn, J. B. *Surf. Sci.* **1986**, 172, 281.
- (15) Coulston, S. W.; Haller, G. L. *J. Chem. Phys.* **1991**, 95, 6932.
- (16) Kunimori, K.; Haller, G. L. *Bull. Chem. Soc. Jpn.* **1992**, 65, 2450.
- (17) Watanabe, K.; Ohnuma, H.; Uetsuka, H.; Kunimori, K. *Surf. Sci.* **1996**, 368, 366.
- (18) Watanabe, K.; Uetsuka, H.; Ohnuma, H.; Kunimori, K. *Catal. Lett.* **1997**, 47, 17.
- (19) Uetsuka, H.; Watanabe, K.; Kimpura, H.; Kunimori, K. *Langmuir* **1999**, 15, 5795.
- (20) Nakao, K.; Hayashi, H.; Uetsuka, H.; Ito, S.; Onishi, H.; Tomishige, K.; Kunimori, K. *Catal. Lett.* **2003**, 85, 213.
- (21) Nakao, K.; Ito, S.; Tomishige, K.; Kunimori, K. *Chem. Phys. Lett.* **2005**, 410, 86.
- (22) Nakao, K.; Ito, S.; Tomishige, K.; Kunimori, K. *Catal. Lett.* **2005**, 103, 179.
- (23) Nakao, K.; Ito, S.; Tomishige, K.; Kunimori, K. *J. Phys. Chem. B* **2005**, 109, 17553.
- (24) Nakao, K.; Ito, S.; Tomishige, K.; Kunimori, K. *J. Phys. Chem. B* **2005**, 109, 17579.
- (25) Nakao, K.; Ito, S.; Tomishige, K.; Kunimori, K. *Catal. Today*, in press.
- (26) Rzeźnicka, I.; Golam Moula, Md.; Morales de la Garza, L.; Ohno, Y.; Matsushima, T. *J. Chem. Phys.* **2003**, 119, 9829.
- (27) Matsushima, T. *Surf. Sci. Rep.* **2003**, 52, 1.
- (28) Bald, D. J.; Kunkel, R.; Bernasek, S. L. *J. Chem. Phys.* **1996**, 104, 7719.
- (29) Bald, D. J.; Bernasek, S. L. *J. Chem. Phys.* **1998**, 109, 746.
- (30) Schmidt, J.; Stuhlmann, Ch.; Ibach, H. *Surf. Sci.* **1993**, 284, 121.
- (31) Tappe, W.; Korte, U.; Meyer-Ehmsen, G. *Surf. Sci.* **1997**, 388, 162.
- (32) Krischer, K.; Eiswirth, M.; Ertl, G. *J. Chem. Phys.* **1992**, 96, 9161.
- (33) McCabe, R. W.; Schmidt, L. D. *Surf. Sci.* **1977**, 66, 101.
- (34) Wartnaby, C. E.; Stuck, A.; Yeo, Y. Y.; King, D. A. *J. Phys. Chem.* **1996**, 100, 12483.
- (35) Ducros, R.; Merrill, R. P. *Surf. Sci.* **1976**, 55, 227.
- (36) Comrie, C. M.; Lambert, R. M. *J. Chem. Soc., Faraday I* **1976**, 72, 1659.
- (37) Monroe, D. R.; Merrill, R. P. *J. Catal.* **1980**, 65, 461.
- (38) Gumhalter, B.; Matsushima, T. *Surf. Sci.* **2004**, 561, 183.
- (39) Alavi, A.; Hu, P.; Deutsch, T.; Silvestrelli, P. L.; Hutter, J. *Phys. Rev. Lett.* **1998**, 80, 3650.
- (40) Petrova, N. V.; Yakovkin, I. N. *Surf. Sci.* **2005**, 578, 162.
- (41) Sharma, R. K.; Brown, W. A.; King, D. A. *Surf. Sci.* **1998**, 414, 68.
- (42) Helveg, S.; Lorensen, H. T.; Hørch, S.; Lægsgaard, E.; Stensgaard, I.; Jacobsen, K. W.; Nørskov, J. K.; Besenbacher, F. *Surf. Sci.* **1999**, 430, L533.
- (43) Hayden, B. E.; Murray, A. J.; Parsons, R.; Pegg, D. J. *J. Electroanal. Chem.* **1996**, 409, 51.
- (44) Zhdanov, V. P. *Surf. Sci.* **1986**, 165, L31.
- (45) Sowa, E. C.; Van Hove, M. A.; Adams, D. L. *Surf. Sci.* **1988**, 199, 174.
- (46) Molinari, E.; Tomellini, M. *Chem. Phys.* **2002**, 277, 373.
- (47) Zhdanov, V. P. *Surf. Sci.* **2005**, 575, 313.